Holistic Joint Optimal Cooperative Spectrum Sensing and Transmission Based on Cooperative Communication in Cognitive Radio

Weizhi Zhong[1], Kunqi Chen[1], Xin Liu [2], Jianjiang Zhou[3]
[1] College of Astronautics, Nanjing University of Aeronautics and Astronautics
Nanjing 210016, Jangsu - P. R. China;
[e-mail: zhongwz@nuaa.edu.cn, kunzinuaa@nuaa.edu.cn]
[2] School of Information and Communication Engineering, Dalian University of Technology
Dalian 116024, Liaoning - P. R. China;
[e-mail: liuxinstar1984@dlut.edu.cn]
[3] College of Electronic and Information Engineering, Nanjing University of Aeronautics and Astronautics
Nanjing 210016, Jangsu - P. R. China;
[e-mail: zjjee@nuaa.edu.cn]
* Corresponding author: Xin Liu

Received August 28, 2016; revised December 12, 2016; revised January 12, 2017; accepted January 13, 2017; published March 31, 2017

Abstract

In order to utilize the licensed channel of cognitive radio (CR) when the primary user (PU) is detected busy, a benefit-exchange access mode based on cooperative communication is proposed to allow secondary user (SU) to access the busy channel through giving assistance to PU's communication in exchange for some transmission bandwidth. A holistic joint optimization problem is formulated to maximize the total throughput of CR system through jointly optimizing the parameters of cooperative spectrum sensing (CSS), including the local sensing time, the pre-configured sensing decision threshold, the forward power of cooperative communication, and the bandwidth and transmission power allocated to SUs in benefit-exchange access mode and traditional access mode, respectively. To solve this complex problem, a combination of bi-level optimization, interior-point optimization and exhaustive optimization is proposed. Simulation results show that, compared with the tradition throughput maximizing model (TTMM), the proposed holistic joint optimization model (HJOM) can make use of the channel effectively even if PU is busy, and the total throughput of CR obtains a considerable improvement by HJOM.

Keywords: Cognitive radio, cooperative spectrum sensing, benefit-exchange access, throughput, bi-level optimization.

This work was supported by the National Natural Science Foundations of China under Grant No. 61601221, the Natural Science Foundations of Jiangsu Province under Grant No. BK20140828, the China Postdoctoral Science Foundations under Grant Nos. 2015M581791 and 2015M580425, and the Fundamental Research Funds for the Central Universities under Grant Nos. DUT16RC(3)045 and NS2017066.

https://doi.org/10.3837/tiis.2017.03.003 **ISSN : 1976-7277**

1. Introduction

To solve the spectrum-scarcity problem, cognitive radio (CR) has been proposed owing to its opportunistic transmission and dynamic spectrum access capabilities in temporal, frequency and spatial domains [1]. In the traditional interweave CR model, secondary user (SU) detects the primary user (PU) state through local spectrum sensing and then only access channels at the absence of the PU [2-4]. However, due to multipath fading, shadowing and hidden terminal problem, reliable spectrum sensing cannot always been guaranteed [5]. Thus, cooperative spectrum sensing (CSS) has been proposed to ameliorate the spectrum sensing performance. In CSS, SUs sense the spectrum independently and then deliver their sensing data to the fusion center that makes the final decision on the PU status [6-8].

Throughput is important to evaluate the performance of a communication system. Therefore, most of previous works focus on jointly optimizing CSS and data transmission to maximize the throughput of the traditional interweave CR mode [9]. In [10], the optimal sensing-throughput tradeoff model is proposed for a single-channel CR system, where the transmission power is supposed to be fixed. The joint optimization of spectrum sensing and dynamic resource allocation for single SU is investigated in [11], and further considering CSS, an upgrade model for the multiple SUs is studied in [12]. Both of the models in [11] and [12] make a significant improvement on the CR throughput.

However, these proposed models are based on the traditional interweave CR mode, whose performances strictly depend on the status of PU. Thus if the idle probability of PU is very low, SU can hardly access the licensed channels, yielding the interrupt of SU communications. Due to the capabilities of increasing diversity gain and power saving in multi-nodes systems, cooperative communication has spurred great interest in recent years [13]. In cooperative communication, several users act as relay nodes to cooperatively forward data between source and destination nodes, which can dramatically ameliorate the outage probability and throughput of source-to-destination channel [14-16]. Some works have considered making use of the licensed spectrum through cooperative communication, even if PU is detected busy. In [17], a scenario with a pair of PU and SU is considered, where the SU acts as a “transparent” relay for the PU transmission link in exchange for more access opportunities. The power allocation at the SU transmitter is investigated and the potential effect on the stable capability of the whole CR system caused by the cooperative communication is discussed. In [18], a joint optimization problem of transmission channel, relay determination and corresponding transmission mode selection is proposed to maximize the outage capability of CR networks. Moreover, a single-user heterogeneous CR network is considered in [19], where SU acts as relay node to help PU communicate via amplify-and-forward (AF) mode while implementing its own communication using some exchanged bandwidth released by the PU. The transmission power allocation strategy is also studied in [18] and [19]. However, all the above researches consider the optimization model unilaterally. The joint optimization of different channel access modes in terms of different PU status has not been considered, such as the joint optimization of CSS and cooperative communication in CR.

In fact, when evaluating the performance of a communication system, the outage probability and the total throughput are the most important metrics while the data transmission bandwidth is not necessary [19]. Therefore, SUs may act as relay nodes to help PU forward data and exchange for some bandwidth released by PU to transmit their own data, thus ameliorating the outage probability of SU while guaranteeing the basic throughput of PU

[17,19]. In this paper, we propose a multi-user benefit-exchange access mode to allow SUs to access the licensed channel at the busyness of the PU. Moreover, once PU is not busy, the traditional access mode is still adopted for the SUs' access. Then, we formulate a holistic joint optimization of CSS in these two different access modes, including sensing time, detection threshold, proportion of bandwidth and homologous transmission power, to maximize the throughput of all SUs.

The rest of paper is organized as follows. In Section 2, the system model is proposed by respectively introducing CSS and the benefit-exchange mode, and the joint optimization model is also formulated. Then, the convexity of this optimization model is illustrated in detail and a combined algorithm of bi-level optimization and interior method is proposed to solve the optimization problem in Section 3. Finally, simulation results and conclusions are demonstrated in Section 4 and 5, respectively.

2. System Model

In this paper, we consider a single channel CR system, which consists of one primary user, N secondary users, and one licensed channel with the bandwidth W. Besides, to implement cooperative communication more effectively, we also assume all SUs are close to the PU receiver, i.e. the channel states, from SUs to the PU receiver, are favorable.

The system is assumed to be strictly synchronized. A time-slot transmission scheme is adopted, where the communication duration is divided into several slots with the same length T. Each slot contains three phases including local spectrum sensing phase, cooperative sensing phase and transmission phase [12]. Through time division multiple access (TDMA), all SUs first sense the PU status independently in local spectrum sensing phase and then deliver their own sensing statistics to the fusion center that makes the final decision on the PU status in cooperative sensing phase, as shown in **Fig. 1**. Finally, in the transmission phase, if PU is decided to be idle by the fusion center, SUs can access the channel by the traditional access mode; otherwise, the proposed benefit-exchange access mode is adopted [20].

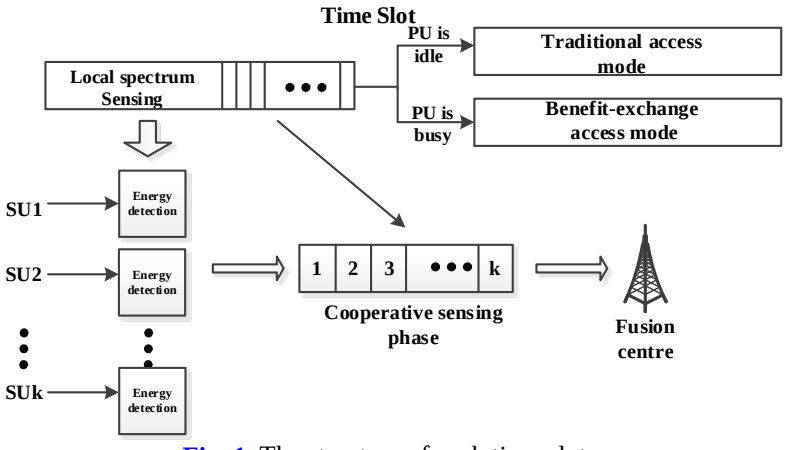

Fig. 1. The structure of each time-slot

2.1. Cooperative Spectrum Sensing

In local sensing phase, each SU senses the PU signal by spanning the licensed channel. Due to the easy implement without any prior knowledge of PU, energy detection has been the most widely used sensing method recently. Energy detection is implemented via comparing the

metrical PU signal energy with a pre-configured decision threshold. If the metrical energy lies above the threshold, the PU status is assumed to be busy; otherwise, the status is judged as idle [10]. The signal received by SU i for $i=1,2,\cdots,N$ in the channel follows a binary hypothesis as [21]

$$y_i(m)=\begin{cases} n(m), & H_0 \\ s(m)h_i^{sr}+n(m), & H_1 \end{cases} \quad m=1,2,\cdots,M \tag{1}$$

where $y_i(m)$ denotes the received sampled signal, H_0 and H_1 denote the idle and busy status of PU, respectively, $s(m)$ is the PU transmission signal with power P_s, $n(m)$ is the Gaussian noise with mean 0 and variance σ^2, h_i^{sr} is the channel gain from the PU transmitter to the SUi receiver. M is the number of sampling nodes as follows

$$M=\tau f_s \tag{2}$$

where τ denotes the local spectrum sensing duration and f_s denotes the sampling frequency. Using energy detection, the metrical PU signal energy of SU i is given as

$$\mathrm{E}(y_i)=\frac{1}{M}\sum_{m=1}^{M}\left|y_i(m)\right|^2 \tag{3}$$

Furthermore, in CSS, the fusion center makes the final decision on PU status via gathering energy statistics from all the local sensing SUs. Thus the final energy statistic obtained by the fusion center is given as follows

$$\Omega=\frac{1}{N}\sum_{i=1}^{N}E(y_i)=\frac{1}{NM}\sum_{i=1}^{N}\sum_{m=1}^{M}\left|y_i(m)\right|^2 \tag{4}$$

Supposing the pre-configured detection threshold is λ, the false alarm and detection probabilities of CSS are formulated, respectively, by following [10] as

$$\begin{cases} Q_f=Q\left(\left(\dfrac{\lambda}{\sigma^2}-1\right)\sqrt{N\tau f_s}\right) \\ Q_d=Q\left(\left(\dfrac{\lambda}{\sigma^2}-\bar{\gamma}-1\right)\sqrt{\dfrac{N\tau f_s}{2\bar{\gamma}+1}}\right) \end{cases} \tag{5}$$

where $\bar{\gamma}=\sum_{i=1}^{N}(P_s\left|h_i^{sr}\right|^2/\sigma^2)\Big/N$ denotes the average sensing SNR of all SUs, and the function $Q(\cdot)$ is defined as

$$Q(x)=\frac{1}{\sqrt{2\pi}}\int_x^{+\infty}\exp\left(-\frac{t^2}{2}\right)\mathrm{d}t \tag{6}$$

To ensure the reliability and stability of the CR system, we further assume that the upper bound of the false alarm probability Q_f should be no larger than 0.5, i.e. $Q_f\le Q_{f\max}\le 0.5$, and the lower bound of the detection probability Q_d is always larger than 0.5, i.e. $Q_d\ge Q_{d\min}\ge 0.5$. Moreover, we only focus on the case that PU is accurately detected.

2.2. Traditional Access Mode

In the transmission phase, once PU is detected idle, each SU is allocated a portion of the licensed channel at a certain transmission power [12]. In this paper, we assume SU i occupies a portion $\omega_i^{\Theta}(0\le\omega_i^{\Theta}\le 1)$ of the channel with a certain transmission power $P_i^{rr\Theta}$, which can be implemented via either orthogonal frequency division multiple access (OFDMA) or Filter Bank Multicarrier (FBMC). Moreover, the channel gain between SU's transmitter and

receiver is denoted by h_i^{rr} . Using the traditional access mode, the SUi's achievable transmission rate is given as

$$C_i^{\Theta} = \omega_i^{\Theta} \cdot \log_2 \left(1 + \frac{P_i^{rr\Theta} \left| h_i^{rr} \right|^2}{\omega_i^{\Theta} \sigma^2} \right) \tag{7}$$

In order to facilitate comparison, we first introduce the traditional throughput maximizing problem proposed in [10]. In this model, SUs can access the licensed channel only when the PU is idle and a joint optimization of CSS, including sensing time and detection threshold, and data transmission, including proportion of transmission power and bandwidth, is formulated to maximize the throughput of all SUs.

We suppose that the cooperative time used by each SU to deliver their local sensing statistics to the fusion center is ξ . By TDMA, the whole cooperative overhead is given as $T_{\mathrm{c}} = N\xi$. Then the length of transmission phase is given as

$$T_t = T - \tau - T_{\mathrm{c}} = T - \tau - N\xi \tag{8}$$

Supposing P_{H0} is the idle probability of PU, the probability that PU is indeed idle and no false alarm appears is $P_{H0}(1-Q_f)$. Therefore, the total throughput of SUs is given as

$$R_t = \frac{T - \tau - N\xi}{T} \sum_{i=1}^{N} \left[P_{H_0} (1 - Q_f(\tau, \lambda)) C_i^{\Theta} \right] \tag{9}$$

The traditional throughput maximizing model model (**TTMM**) is formulated from [10] as

$$\begin{aligned} \max_{\tau, \lambda, \omega_i^{\Theta}, P_i^{rr\Theta}} \; & R^{all} = \frac{T - \tau - N\xi}{T} \left[P_{H0} \left(1 - Q_f(\tau, \lambda)\right) \sum_{i=1}^{N} \omega_i^{\Theta} \cdot \log_2 \left(1 + \frac{P_i^{rr\Theta} \left| h_i^{rr} \right|^2}{\omega_i^{\Theta} \sigma^2} \right) \right] \\ \text{s.t.} \quad & 0 \le \tau \le T - N\xi \\ & 0 \le Q_f \le Q_{f\max} \le 0.5, \; 0.5 \le Q_{d\min} \le Q_d \le 1 \\ & 0 < \sum_{i=1}^{N} \omega_i^{\Theta} < 1, \qquad \omega_i^{\Theta} > 0 \text{ for } i = 1, 2, \cdots N \\ & 0 \le P_i^{rr\Theta} \le P_{\max}, \quad i = 1, 2 \cdots, N \end{aligned} \tag{10}$$

where $P_{\max}$ is the maximal transmission power of SUs.

2.3. Holistic Joint Optimization Model

To make use of the licensed channel while PU is busy, we take cooperative communication into consideration and propose a multi-user benefit-exchange access model for a multi-user CR system. In this model, all SUs assist to relay PU's transmission data and thus exchange for some bandwidth released by PU to implement their own communications. It is worth mentioning that cooperative communication can remarkably increase the diversity gain of the system and ameliorate the outage probability well [18, 22]. Therefore, if SUs are available to assist PU's communication, PU may release some bandwidth for SUs' own communications as a benefit exchange while guaranteeing its previous throughput level. To avoid violating the privacy of PU's communication, we utilize AF rather than decode-and forward (DF) to forward PU's transmission data [19]. The detailed structure of benefit-exchange access mode is proposed in **Fig. 2**. We suppose the channel state information (CSI) of the system is obtained via channel estimation and broadcast to all the users in advance. Besides, we also assume CSI keeps constant in one time slot. Thus, the specific configuration of the access

mode can be finalized at the beginning of the transmission phase. Meanwhile, maximum-ratio combining (MRC) can be used by the PU receiver to decode the received mixed PU signal consisting of the signals forwarded by SUs and the directional PU signal. Note that the data forwarded by all the SUs, i.e. the PU transmission data, are all the same. Thus all SUs can simultaneously forward the PU data in the same frequency band and the weight coefficients of MRC can be multiplied at the transmitters of SUs and PU beforehand.

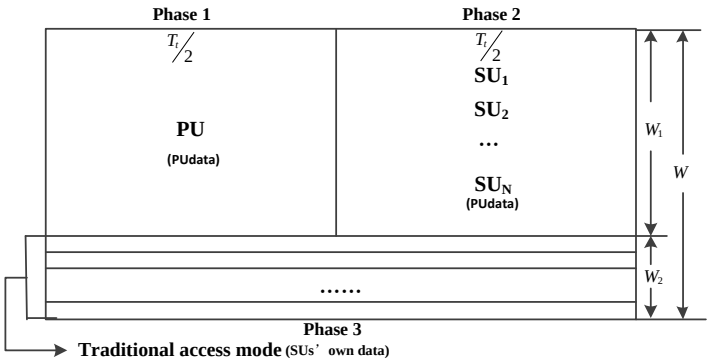

Fig. 2. The structure of Benefit-exchange Access Mode

In **Fig. 2**, the access mode consists of three phase, including PU broadcast phase 1, SU relay phase 2 and SU communication phase 3. In Phase 1, PU broadcast its communication data to its own receiver and all SUs with a bandwidth W_1 during $T_t/2$, and then in Phase 2, PU terminates its own broadcast and all SUs transmit their PU data, received in Phase 1, to the PU receiver. Actually, Phase 1 and Phase 2 can be easily implemented via TDMA. As an exchange, PU releases a bandwidth $W_2 = W - W_1$ for SUs to transmit their own data in Phase 3, and the traditional access mode is utilized to assign the released channel. Following the methods in Section 2.2 and Section 2.3, the ith SU's achievable transmission rate in the benefit-exchange access mode can be formulated as

$$C_i^* = \omega_i^* \cdot \log_2\left(1 + \frac{P_i^{rr*}\left|h_i^{rr}\right|^2}{\omega_i^* \sigma^2}\right) \tag{11}$$

where ω_i^* is the assigned bandwidth of SU i with a certain transmission power P_i^{rr*} in benefit-exchange access mode. Furthermore, the total throughput of all SUs in the benefit-exchange access mode can be formulated as

$$R_e = \frac{T - \tau - N\xi}{T} \sum_{i=1}^{N} \left[P_{H1} \cdot Q_d(\tau, \lambda) C_i^* \right] \tag{12}$$

To impel PU to release the bandwidth, we must ensure that PU's throughput in the benefit-exchange access mode is no less than PU's previous throughput, i.e.

$$R_{PU}^{now} \geq R_{PU}^{pre.} = \frac{T_t}{T} \log_2\left(1 + \frac{P_s\left|h^{sd}\right|^2}{\sigma^2}\right) \tag{13}$$

where h^{sd} denotes the channel gain from PU's transmitter to its own receiver. Following the ways in [19], the throughput of PU in benefit-exchange access mode can be given as

$$R_{PU}^{now}=\frac{T_t}{2T}W^*\log_2\left(1+\frac{P_s\left|h^{sd}\right|^2}{W^*\sigma^2}+\sum_{i=1}^{N}\frac{P_s\left|h_i^{sr}\right|^2\cdot P^{rd}\left|h_i^{rd}\right|^2}{\left(P_s\left|h_i^{sr}\right|^2+P^{rd}\left|h_i^{rd}\right|^2+W^*\sigma^2\right)\cdot W^*\sigma^2}\right) \tag{14}$$

where h_i^{rd} denotes the channel gain from ith SU's transmitter to PU's receiver, P^{rd} denotes the power cost by each SU to forward the PU data and $W^*=1-\sum_{i=1}^{N}\omega_i^*$ is the portion of bandwidth used for cooperative communication. To ensure the fairness, we assume the forward-cost powers of all SUs are all the same. Hence, the total throughput of the all the SUs is given by

$$R^{all}=\frac{T-\tau-N\xi}{T}\left[P_{H0}(1-Q_f)\sum_{i=1}^{N}\omega_i^{\Theta}\log_2\left(1+\frac{P_i^{rr\Theta}\left|h_i^{rr}\right|^2}{\omega_i^{\Theta}\sigma^2}\right)+P_{H1}Q_d\sum_{i=1}^{N}\omega_i^*\log_2\left(1+\frac{P_i^{rr*}\left|h_i^{rr}\right|^2}{\omega_i^*\sigma^2}\right)\right] \tag{15}$$

Therefore, catering to different PU status, the holistic joint optimization model (**HJOM**) of CSS and different access modes to maximize the throughput of all SUs can be formulated as follows

$$\begin{aligned}
&\max_{\substack{\tau,\lambda,p^{rd},W^*\\ \boldsymbol{\omega}^{\Theta},\mathbf{P}^{\mathbf{rr}\Theta},\boldsymbol{\omega}^*,\mathbf{P}^{rr*}}} \quad R^{all}\left(\tau,\lambda,p^{rd},W^*,\ \boldsymbol{\omega}^{\Theta},\mathbf{P}^{\mathbf{rr}\Theta},\boldsymbol{\omega}^*,\mathbf{P}^{rr*}\right)\\
&\text{s.t.}\ \ (a)\ \ 0\le\tau\le T-N\xi\\
&\qquad (b)\ \ 0\le Q_f\le 0.5\\
&\qquad (c)\ \ 0.5\le Q_d\le 1\\
&\qquad (d)\ \ 0<\sum_{i=1}^{N}\omega_i^{\Theta}<1\,, \qquad \omega_i^{\Theta}>0 \text{ for } i=1,2,\cdots N\\
&\qquad (e)\ \ 0\le P_i^{rr\Theta}\le P_{\max}\,, \qquad i=1,2\cdots,N\\
&\qquad (f)\ \ 0<W^*=1-\sum_{i=1}^{N}\omega_i^*<1, \quad \omega_i^*>0 \text{ for } i=1,2,\cdots N\\
&\qquad (g)\ \ P_i^{rr*}+P^{rd}\le P_{\max}\,, \qquad i=1,2\cdots,N\\
&\qquad (h)\ \ R_{PU}^{now}\ge R_{PU}^{pre.}
\end{aligned} \tag{16}$$

where $P_{\max}$ denotes the maximal transmission power of each SU.

3. Holistic Joint Throughout Optimization Algorithm

To solve problem (16), we implement the bi-level optimization where (16) is divided into two sub-level optimization problem. Specifically, the upper-level is to optimize W^*, while the lower-level is to optimize other parameters with a specific W^*. The lower-level optimization problem is given as

$$\begin{aligned}
&\max_{\substack{\tau,\lambda,p^{rd}\\ \boldsymbol{\omega}^{\Theta},\mathbf{P}^{\mathbf{rr}\Theta},\boldsymbol{\omega}^*,\mathbf{P}^{rr*}}} \quad R^{all}\\
&\text{s.t.}\quad \text{cons. (16a)-(16h)}
\end{aligned} \tag{17}$$

and the upper-level one is given as

$$\begin{aligned}
&\max_{W^*} \quad R^{all}\\
&\text{s.t.}\quad \text{cons. (16h)}
\end{aligned} \tag{18}$$

Actually, when W^* is given, problem (17) is a convex optimization problem and can be directly solved by the interior-point method. Next, we will prove this convexity in detail. For a given W^*, we give three lemmas as follows.

Lemma 1: Functions $Q_f(\tau,\lambda)$ and $Q_f(\tau,\lambda)$ is concave and convex in both τ and λ, respectively.

Proof: With a specific λ, we derive the first and second derivations of $Q_f(\tau,\lambda)$ and $Q_d(\tau,\lambda)$ in τ, respectively, as follows

$$\begin{cases} \dfrac{\partial Q_f(\tau)}{\partial \tau} = -\dfrac{\left(\dfrac{\lambda}{\sigma^2}-1\right)\sqrt{Nf_s}}{2\sqrt{2\pi\tau}}\exp\left(-\dfrac{\left(\dfrac{\lambda}{\sigma^2}-1\right)^2 N\tau f_s}{2}\right) \\ \dfrac{\partial Q_d(\tau)}{\partial \tau} = -\dfrac{\left(\dfrac{\lambda}{\sigma^2}-\overline{\gamma}-1\right)\sqrt{Nf_s}}{2\sqrt{(4\overline{\gamma}+2)\pi\tau}}\exp\left(-\dfrac{\left(\dfrac{\lambda}{\sigma^2}-\overline{\gamma}-1\right)^2 N\tau f_s}{4\overline{\gamma}+2}\right) \end{cases} \tag{19}$$

$$\begin{cases} \dfrac{\partial^2 Q_f(\tau)}{\partial \tau^2} = \dfrac{\left(\dfrac{\lambda}{\sigma^2}-1\right)\left(\left(\dfrac{\lambda}{\sigma^2}-1\right)^2 Nf_s+\dfrac{1}{\tau}\right)\sqrt{Nf_s}}{4\sqrt{2\pi\tau}}\exp\left(-\dfrac{\left(\dfrac{\lambda}{\sigma^2}-1\right)^2 N\tau f_s}{2}\right) \\ \dfrac{\partial^2 Q_d(\tau)}{\partial \tau^2} = \dfrac{\left(\dfrac{\lambda}{\sigma^2}-\overline{\gamma}-1\right)\left(\left(\dfrac{\lambda}{\sigma^2}-\overline{\gamma}-1\right)^2 \dfrac{Nf_s}{2\overline{\gamma}+1}+\dfrac{1}{\tau}\right)\sqrt{Nf_s}}{4\sqrt{(4\overline{\gamma}+2)\pi\tau}}\exp\left(-\dfrac{\left(\dfrac{\lambda}{\sigma^2}-\overline{\gamma}-1\right)^2 N\tau f_s}{4\overline{\gamma}+2}\right) \end{cases} \tag{20}$$

From cons. (16b) and (16c), we have

$$1 \le \frac{\lambda}{\sigma^2} \le \overline{\gamma}+1 \tag{21}$$

By substituting (21) into (19) and (20), we further have

$$\frac{\partial Q_f(\tau)}{\partial \tau} \le 0, \frac{\partial Q_d(\tau)}{\partial \tau} \ge 0, \frac{\partial^2 Q_f(\tau)}{\partial \tau^2} \ge 0, \ \frac{\partial^2 Q_d(\tau)}{\partial \tau^2} \le 0 \tag{22}$$

Therefore, with a specific λ, $Q_f(\tau,\lambda)$ is concave and $Q_d(\tau,\lambda)$ is convex with respect to τ. Next, with a specific τ, we derive the first and second derivations of $Q_f(\tau,\lambda)$ and $Q_d(\tau,\lambda)$ in λ, respectively, as follows

$$\frac{\partial Q_f(\lambda)}{\partial \lambda} = -\frac{\sqrt{N\tau f_s}}{\sqrt{2\pi}\sigma^2}\exp\left(-\frac{\left(\dfrac{\lambda}{\sigma^2}-1\right)^2 N\tau f_s}{2}\right) \tag{23}$$

$$\frac{\partial Q_d(\lambda)}{\partial \lambda} = -\frac{\sqrt{N\tau f_s}}{\sqrt{(4\overline{\gamma}+2)\pi\sigma^2}} \exp\left(-\frac{\left(\frac{\lambda}{\sigma^2} - \overline{\gamma} - 1\right)^2 N\tau f_s}{4\overline{\gamma}+2} \right) \tag{24}$$

$$\frac{\partial^2 Q_f(\lambda)}{\partial \lambda^2} = \frac{\left(\frac{\lambda}{\sigma^2} - 1\right)\left(N\tau f_s\right)^{3/2}}{\sqrt{2\pi}\sigma^4} \exp\left(-\frac{\left(\frac{\lambda}{\sigma^2} - 1\right)^2 N\tau f_s}{2} \right) \tag{25}$$

$$\frac{\partial^2 Q_d(\lambda)}{\partial \lambda^2} = \frac{\left(\frac{\lambda}{\sigma^2} - \overline{\gamma} - 1\right)\left(\frac{N\tau f_s}{2\overline{\gamma}+1}\right)^{3/2}}{\sqrt{2\pi}\sigma^4} \exp\left(-\frac{\left(\frac{\lambda}{\sigma^2} - \overline{\gamma} - 1\right)^2 N\tau f_s}{4\overline{\gamma}+2} \right) \tag{26}$$

By substituting (21) into (23), (24), (25) and (26) we further have

$$\frac{\partial Q_f(\lambda)}{\partial \lambda} \le 0, \frac{\partial Q_d(\lambda)}{\partial \lambda} \le 0, \frac{\partial^2 Q_f(\lambda)}{\partial \lambda^2} \ge 0, \ \frac{\partial^2 Q_d(\lambda)}{\partial \lambda^2} \le 0 \tag{27}$$

Similarly, with a specific τ, $Q_f(\tau,\lambda)$ is concave and $Q_d(\tau,\lambda)$ is convex in λ. This completes the proof.

Lemma 2: The objective function of problem (17) is a convex function.

Proof 2: For simplification, we first let

$$\begin{gathered} A = \frac{T-\tau-N\xi}{T} P_{H0}(1-Q_f), \quad B = \frac{T-\tau-N\xi}{T} P_{H1} Q_d, \\ P_\Theta = \frac{P_i^{rr\Theta}\left|h_i^{rr}\right|^2}{\sigma^2}, P_* = \frac{P_i^{rr*}\left|h_i^{rr}\right|^2}{\sigma^2}, \omega_\Theta = \frac{\left|h_i^{rr}\right|^2}{\omega_i^\Theta \sigma^2}, \omega_* = \frac{\left|h_i^{rr}\right|^2}{\omega_i^* \sigma^2} \end{gathered} \tag{28}$$

Thus, when other parameters are given, the second derivation of R_{all} in ω_i^Θ is given as

$$\frac{\partial^2 R^{all}(\omega_\Theta)}{\partial {\omega_\Theta}^2} = \frac{AP_\Theta}{(\omega_i^\Theta + P_\Theta)\ln 2}\left(\frac{1}{\omega_i^\Theta + P_\Theta} - \frac{1}{\omega_i^\Theta}\right) \le 0 \tag{29}$$

i.e., R^{all} is convex in ω_i^Θ. Similarly, we also have

$$\frac{\partial^2 R^{all}(p_i^{rr\Theta})}{\partial (P_i^{rr\Theta})^2} = -\frac{A\omega_\Theta \left|h_i^{rr}\right|^2}{(1+\omega_\Theta P_i^{rr\Theta})^2 \sigma^2 \ln 2} \le 0 \tag{30}$$

i.e., R^{all} is also convex in $P_i^{rr\Theta}$. As ω_i^* and P_i^{rr*} have the same forms with ω_i^Θ and $P_i^{rr\Theta}$, respectively, we can also have a similar conclusion that R^{all} is also convex with respect to ω_i^* and P_i^{rr*}. Next, when other parameters are given, we derive the second derivations of R^{all} in τ and λ, respectively, as follows

$$\begin{gathered} \frac{\partial^2 R^{all}(\tau)}{\partial \tau^2} = \frac{2}{T}\left[\left(P_{H_0}\sum_{i=1}^{N} C_i^\Theta\right)\frac{\partial Q_f}{\partial \tau} - \left(P_{H_1}\sum_{i=1}^{N} C_i^*\right)\frac{\partial Q_d}{\partial \tau}\right] - \\ \frac{T-\tau-N\xi}{T}\left[\left(P_{H_0}\sum_{i=1}^{N} C_i^\Theta\right)\frac{\partial^2 Q_f}{\partial \tau^2} - \left(P_{H_1}\sum_{i=1}^{N} C_i^*\right)\frac{\partial^2 Q_d}{\partial \tau^2}\right] \end{gathered} \tag{31}$$

$$\frac{\partial^2 R^{all}(\lambda)}{\partial \lambda^2} = -\frac{T-\tau-N\xi}{T}\left[\left(P_{H_0}\sum_{i=1}^{N} C_i^{\Theta}\right)\frac{\partial^2 Q_f}{\partial \lambda^2} - \left(P_{H_1}\sum_{i=1}^{N} C_i^{*}\right)\frac{\partial^2 Q_d}{\partial \lambda^2}\right] \tag{32}$$

By substituting (22) and (27) in to (31) and (32), we have

$$\frac{\partial^2 R^{all}(\tau)}{\partial \tau^2} \le 0,\ \frac{\partial^2 R^{all}(\lambda)}{\partial \lambda^2} \le 0 \tag{33}$$

i.e., R^{all} is also convex with respect to τ and λ. This completes the proof.

Lemma 3: With a specific W^*, the constraint (16h) is a convex constraint in P^{rd}.

Proof: For a given W^*, we first define

$$\begin{aligned} &H_i^1 = P_s\left|h_i^{sr}\right|^2\left|h_i^{rd}\right|^2,\quad H_i^2 = \left|h_i^{rd}\right|^2 W^*\sigma^2, \\ &H_i^3 = \left(P_s\left|h_i^{sr}\right|^2 + W^*\sigma^2\right)\cdot W^*\sigma^2,\ S = \frac{P_s\left|h^{sd}\right|^2}{\sigma^2} \end{aligned} \tag{34}$$

Thus, $R^{\triangle}(P^{rd})$ can be concisely given as

$$R^{\triangle}(P^{rd}) = \frac{W^*}{2}\log_2\left(1+\frac{S}{W^*}+\sum_{i=1}^{N}\frac{P^{rd}H_i^1}{P^{rd}H_i^2+H_i^3}\right) - \log_2(1+S) \tag{35}$$

The second derivation of $R^{\triangle}$ with respect to P^{rd} can be given as

$$\frac{\partial^2 R^{\triangle}(P^{rd})}{\partial^2 P^{rd}} = -\frac{W^*}{2}\frac{2\left(1+\frac{S}{W^*}+\sum_{i=1}^{N}\frac{P^{rd}H_i^1}{P^{rd}H_i^2+H_i^3}\right)\sum_{i=1}^{N}\frac{H_i^1H_i^2H_i^3}{\left(P^{rd}H_i^2+H_i^3\right)^3} + \left(\sum_{i=1}^{N}\frac{H_i^1H_i^3}{\left(P^{rd}H_i^2+H_i^3\right)^2}\right)^2}{\left(1+\frac{S}{W^*}+\sum_{i=1}^{N}\frac{p^{rd}H_i^1}{P^{rd}H_i^2+H_i^3}\right)^2\ln 2} < 0 \tag{36}$$

i.e. $R^{\triangle}$ is a convex function in P^{rd} and thus the constraint (16h) is a convex constraint in P^{rd} when W^* is given. This completes the proof.

Finally, it is obvious that other constraints of problem (17), i.e. from (16d) to (16g) and (16a), are all linear constraints. Therefore, according to the three lemmas proposed above, when W^* is given, problem (17) is proved to be a convex optimization problem with respect to all other optimization parameters, and thus can be directly solved via the interior-point method [23, 24]. For problem (18), the direct optimization of W^* is intractable. However, the domain of W^* within [0, 1] is a finite set of real number, and thus we consider adopting the exhaustive method to optimize problem (18). As long as the selected exhaustive step ε is small enough, we can also obtain a favorable sub-optimal solution of problem (18). In a word, the combined optimization algorithm, including bi-level optimization, interior-point method and exhaustive method, for problem (16) can be given in the **Algorithm 1**, where $\lfloor 1/\varepsilon \rfloor$ denotes the maximal integer no larger than $1/\varepsilon$.

Algorithm 1. Combined optimization algorithm

Initialization: set an exhaustive step ε and then define a vertex set $\boldsymbol{T} = \{T_k\}_{k=1}^{\lfloor 1/\varepsilon \rfloor}$
(1) For $k = 1, 2, \cdots, \lfloor 1/\varepsilon \rfloor$, repeat step (3) to (4);
(2) Given $W^* = k\varepsilon$, find the optimal solution $\left(\tau_k, \lambda_k, p_k^{rd}, \boldsymbol{\omega}_k^{\Theta}, \boldsymbol{p}_k^{rr\Theta}, \boldsymbol{\omega}_k^*, \boldsymbol{p}_k^{rr*}\right)$ and the corresponding maximal R_k^{all} of the problem (17) via interior-point method;
(3) Let $T_k = \left(\tau_k, \lambda_k, p_k^{rd}, \boldsymbol{\omega}_k^{\Theta}, \boldsymbol{p}_k^{rr\Theta}, \boldsymbol{\omega}_k^*, \boldsymbol{p}_k^{rr*}, W_k^* = k\varepsilon, R_k^{all}\right)$ and add it to $\boldsymbol{T}$;
(4) Find $k^* = \arg\max R_k^{all}$ for $k = 1, 2, \cdots \lfloor 1/\varepsilon \rfloor$ and output T_{k^*}.

4. Simulation Results

In this section, simulation results are proposed to demonstrate the effectiveness of our scheme, by comparing the HJOM, i.e. problem (16), with the TTMM, i.e. problem (10).

We consider a single-PU multi-SU CR network consisting of *N*=8 SUs and one licensed channel with the bandwidth $W = 1$ kHz . The length of the divided time slot is $T = 2$s and the sensing sampling frequency is $f_s = 2$ kHz . The length of cooperative slot used by each SU to deliver sensing data is $\xi = 0.01$ s . The power of the noise is $\sigma^2 = 0.1$W , the transmission power of PU is $P_s = 0.5$W and the maximal transmission power of each SU is $P_{\max} = 0.5$W . The busy and idle probabilities of the licensed channel are $P_{H_1} = P_{H_0} = 0.5$, respectively. The upper bound of the false alarm probability and the lower bound of the detection probability are $Q_{f\max} = Q_{d\min} = 0.5$, respectively. The exhaustive step is $\varepsilon = 10^{-3}$. To operate CSS and cooperative communication more effectively, we consider the circumstance where the channel states from PU's transmitter to SUs' receiver is unfavorable but the channel states from SUs' transmitter to PU's receiver is fine. We define the channel SNR as the square of channel gain to the noise power ratio. We suppose the channel SNR of PU's directional link (PPSNR) is 0 dB/W. Besides, the channel SNR from PU's transmitter to each SU's receiver (PSSNR), the channel SNR from each SU's transmitter to PU's receiver (SPSNR) and the channel SNR of SUs' own communications channel (SSSNR) are respectively given as follows

Table 1. Different channel SNR in the CR network

SUs	1	2	3	4	5	6	7	8
PSSNR(dB/W)	-4	-4	-5	-8	-8	-10	-11	-12
SPSNR(dB/W)	21	29	20	27	28	28	20	23
SSSNR(dB/W)	24	20	29	22	24	24	23	29

First, we demonstrate the effect on the total throughput R^{all} of HJOM caused by the local sensing time τ and the pre-configured sending threshold λ . With different pairs of τ and λ , the optimal utilities of HJOM can be obtained via a simplified **Algorithm 1** including both the exhaustive and inter-point methods. **Fig. 3 (a)** and **(b)** shows R^{all} versus τ and λ via 3D and 2D, respectively, and the global optimal solution obtained by **Algorithm 1** is marked in **Fig. 3 (b)**. It shows that the relation surface is convex, which verifies the proposed lemmas well. Algorithm 1 successfully obtains the optimal solution to maximize R^{all} , and specifically, the optimal $R^{all} = 5.3102$ bps/Hz is obtained when $\tau = 0.0739$ s and $\lambda = 0.1069$. **Fig. 3 (c)** and **(d)**, which show R^{all} versus τ with different λ and versus λ with different τ in detail, are some

particular cross-sections of **Fig. 3 (a)**. Both of them confirm the convexity of (16) and the effectiveness of **Algorithm 1** more concretely. **Fig. 3 (c)** shows with the increase of τ, all the optimal utilities first increase and then decrease. In fact, the increase of τ leads to a lower false alarm probability and a higher detection probability, which imply a better spectrum sensing performance and thus a higher throughput of the whole system. However, the increase of τ also yields the loss of transmission time T_t. Once τ reaches a certain value, the improvement on the spectrum sensing capability is wearing off while the loss of T_t becomes dominant, thus directly triggering the decrease of R^{all}. In **Fig. 3 (d)**, with the increase of λ, R^{all} also first increases and then decrease. Actually, the increase of λ leads to both lower false alarm and detection probabilities. Thus, the first increase of R^{all} is mainly due to the decrease of Q_f, and once λ reaches a certain value, the decrease of Q_d is dominant and finally leads to the decrease of R^{all}. Note that the effect caused by the tradeoff of Q_f and Q_d is mainly determined by the values of the attainable transmission rates of these two access mode, i.e. C^{Θ} and C^{*}.

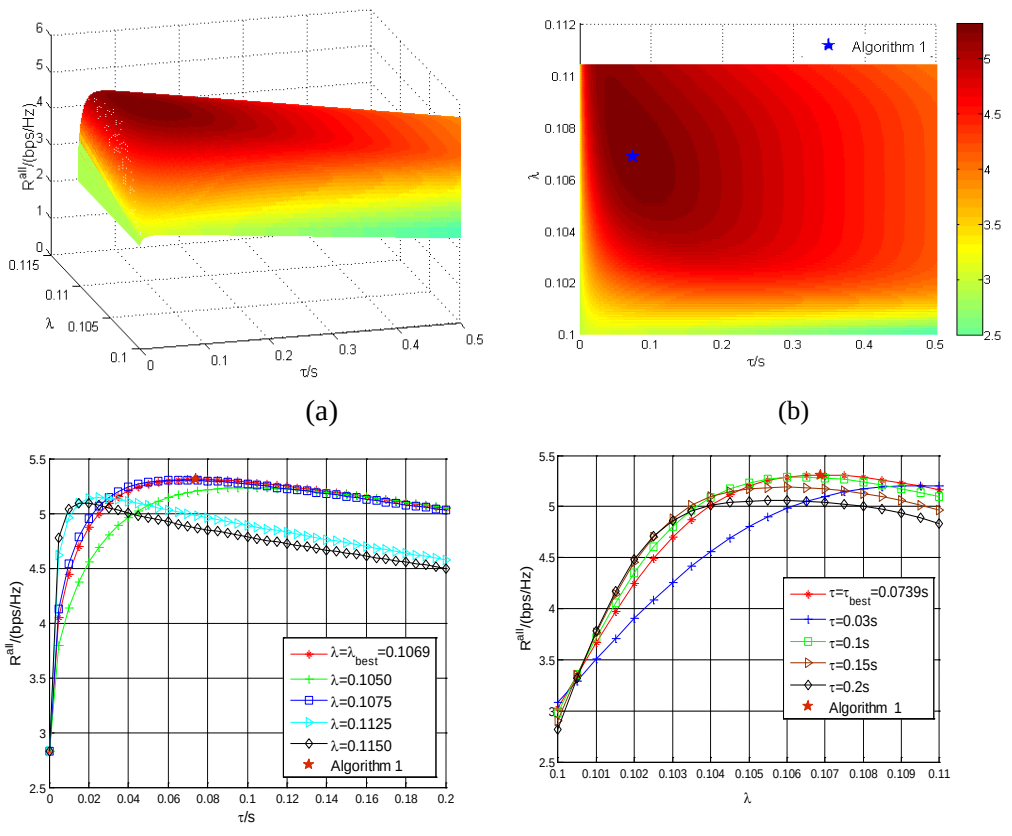

Fig. 3. Effect of τ and λ on R^{all} in HJOM: (a) R^{all} versus τ and λ (3D); (b) R^{all} versus τ and λ (2D); (c) R^{all} versus τ with different λ; (d) R^{all} versus λ with different τ.

Before the detailed simulation analysis of HJOM and TTMM, we compare the computational complexity between these two models first. The 'fmincon' function of Matlab is used to accomplish the interior-point method, which is the most important factor to

influence the computational complexity of the proposed optimization algorithm. Therefore, the complexity can be approximately represented by the running durations of the entire Matlab programs. Fig.4 shows the comparison of algorithm running durations between HJOM and TTMM. We run the Matlab programs for 1000 times to ensure the universality of the comparison. In Fig.4, almost all of the red dots are above the corresponding blue dots, which means that the running durations of HJOM are larger than that of TTMM. In other words, the computational complexity of HJOM is indeed higher than that of TTMM, which is obviously due to the extra cost of BEAM. However, from Fig.4 we can also find that the difference of HJOM and TTMM is very small. Compared with the throughput benefit of HJOM, the slight cost of computational complexity is actually negligible.

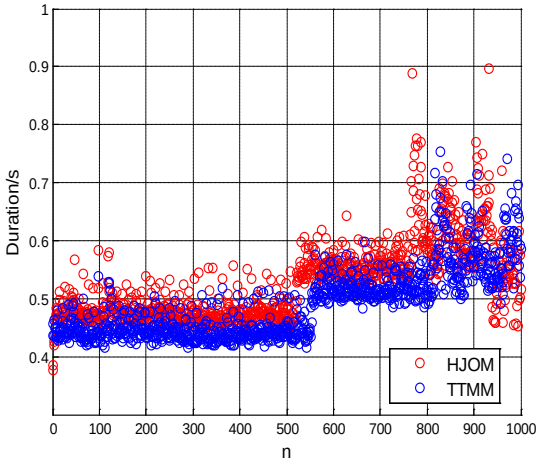

Fig. 4. Comparison of algorithm running durations between HJOM and TTMM (1000 times)

Then, we focus on the effect on both the throughputs in the HJOM and TTMM caused by the original PU transmission power P_s. **Fig. 5 (a)** shows R^{all} versus P_s in both HJOM and TTMM. It can be seen that, with the increase of P_s, the throughput of TTMM keeps increasing all the time. According to **Fig. 5 (c)** and **(d)**, in TTMM, the increase of P_s leads to the sustained decrease of Q_f while Q_d keeps fixed with $Q_{d\min} = 0.5$, which is coincident with the conclusions in [10] and [11]. Thus, the continuous increase of R^{all} in TTMM is mainly due to the decrease of Q_f. In **Fig. 5 (a)**, the curve of R^{all} in HJOM first increases and then decrease. After P_s reaches 0.6W, the optimal utilities of both HJOM and TTMM become same. According to Fig.4 (c) and (d), with the increase of P_s, Q_f keeps decrease while Q_d first increase and then experiences a drastic decrease in HJOM. The increases of Q_f and Q_d are caused by the enhancement of the received PU signal power, which can directly improve the spectrum sensing capability. However, according to (15), the increase of P_s also implies that more cooperative power P^{rd} should be used by SUs to forward PU's communication data to help PU reach the original throughput of PU's directional link. Therefore, the throughput of benefit-exchange access mode, i.e. C^*, is wearing off. As shown in **Fig. 5 (b)**, after P_s reaches 0.6W, even if SUs allocate all transmission power to forward PU's data, it will also be invalid for SUs to help PU achieve its original throughput, and thus C^* becomes zero ultimately. Meanwhile, the HJOM also degenerate into TTMM for the same reason, and thus all contrast curves of HJOM and TTMM in **Fig. 5 (a)**, **(c)** and **(d)** become overlapping after P_s reaches

0.6W. From **Fig. 5 (a)**, we can also find that the throughput of HJOM is always no lower than that of TTMM, which verifies the principle of our work perfectly.

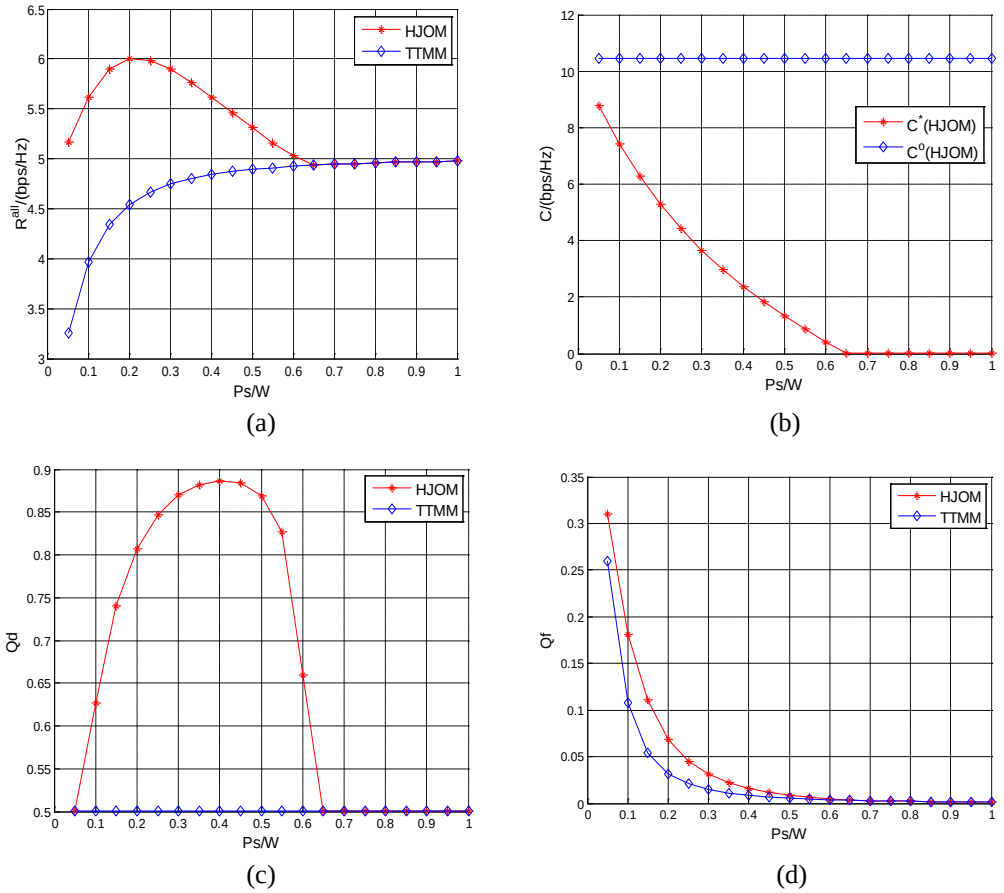

Fig. 5. Effect of P_s on HJOM and TTMM: (a) R^{all} versus P_s in different models; (b) C^{Θ} and C^* of HJOM versus P_s; (c) Q_d versus P_s in different models; (d) Q_f versus P_s in different models.

Next, we focus on the effect on both the throughputs in HJOM and TTMM caused by different configurations of the lower bound of detection probability, i.e. $Q_{d\min}$. **Fig. 6 (a)** shows R^{all} versus $Q_{d\min}$ in both two models. With the increase of $Q_{d\min}$, R^{all} of TTMM keeps decreasing. According to **Fig. 6 (a)**, through replacing Q_f with an expression of Q_d, R^{all} of TTMM can be proved to be a monotonically decreasing function in $Q_{d\min}$ as detailed in [10-12]. Besides, the optimal utilities of TTMM can only be obtained when Q_d acquires its lower bound, i.e. $Q_d = Q_{d\min}$, which is coincident with the TTMM Q_d curves in **Fig. 6 (b)**. For HJOM, with the increase of $Q_{d\min}$, both R^{all} and Q_d keep unchanged at first as shown in **Fig. 6**. However, when $Q_{d\min}$ is larger than a certain value, i.e. almost 0.87, R^{all} begins decreasing and Q_d is always equal to its lower bound $Q_{d\min}$. At the beginning, the optimal Q_d of HJOM is 0.87 and $Q_{d\min}$ has not reached this optimal value, and thus the increase of $Q_{d\min}$ has no influence on the optimization model at first, as shown in **Fig. 6 (b)**. Nevertheless, once $Q_{d\min}$ is larger than

0.87, more and more local sensing time τ should be allocated to satisfy the increase of Q_d, which directly leads to the decrease of transmission time T_t and thus the later decrease of R^{all}, as shown in **Fig. 6(c)**.

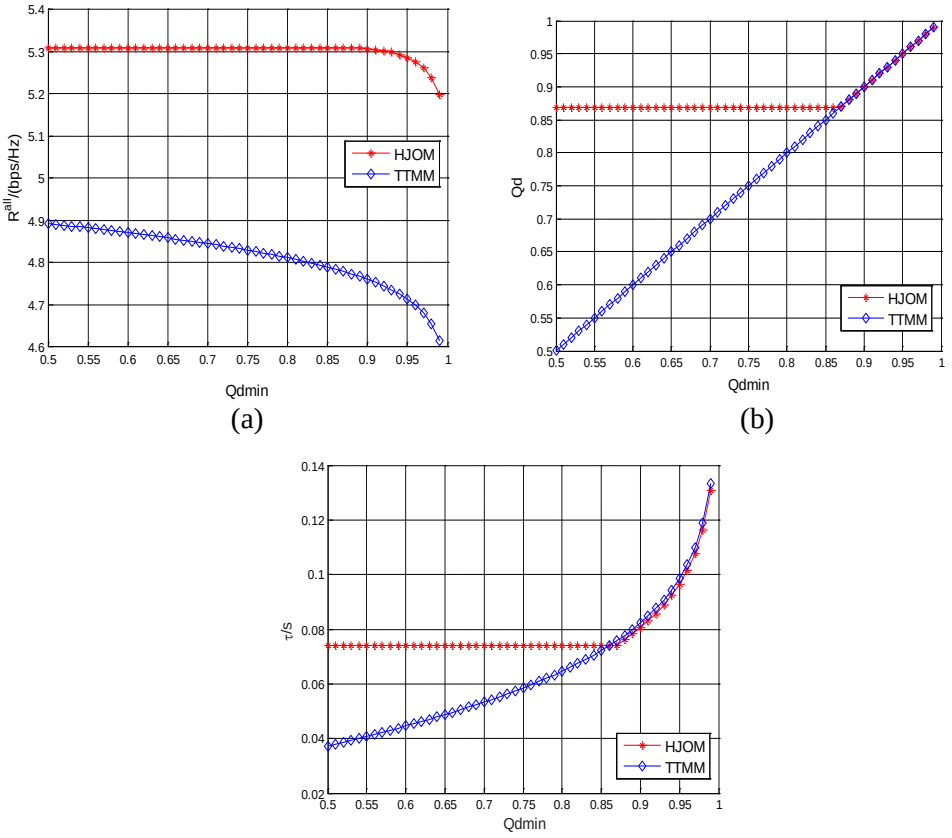

Fig. 6. Effect of $Q_{d\min}$ on HJOM and TTMM: (a) R^{all} versus $Q_{d\min}$ in different models; (b) Q_d versus $Q_{d\min}$ in different model; (c) τ versus $Q_{d\min}$ in different models.

Finally, we demonstrate the effect on these two models caused by the value of P_{H_0}. From **Fig. 7**, it is obvious that with the increase of P_{H_0}, R^{all} of both HJOM and TTMM also keep increasing. R^{all} of HJOM is always larger than that of TTMM, which verifies forcefully the effectiveness of HJOM when using the licensed channel even if PU is busy. Besides, the difference between HJOM and TTMM is decreasing along with the increase of P_{H_0}. Actually, the superiority of HJOM is mainly owing to the spectrum utilization at the presence of PU, and thus the superiority is wearing off when the busy probability of PU is decreasing.

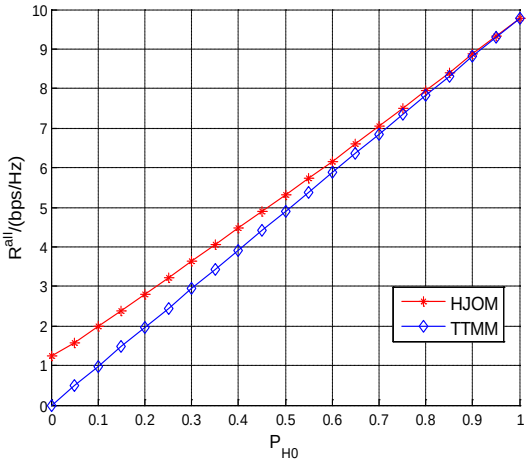

Fig. 7. Effect of P_{H_0} on HJOM and TTMM

5. Conclusion

In this paper, a multi-user benefit-exchange access mode is proposed to allow the SUs to make use of the licensed channel when PU is busy. A holistic joint optimization problem is formulated to maximize the total throughput of CR system via jointly optimizing the parameters of CSS in both benefit-exchange access mode and traditional access mode. A combination of bi-level optimization, interior-point optimization and exhaustive searching is proposed to solve the proposed optimization problem effectively. Finally, we demonstrate the effectiveness of HJOM by comparing it with TTMM. Simulation results show that HJOM has a significant improvement on the total throughput of the CR system and utilizes the licensed channel successfully when PU is detected to be busy

References

[1] X. Chen, H.H. Chen, W. Meng, "Cooperative Communications for Cognitive Radio Networks — From Theory to Applications," *IEEE Communications Surveys & Tutorials*, vol. 16, no. 3, pp 1180-1192, 2014. Article (CrossRef Link)

[2] H. Sun, A. Nallanathan, C. Wang, Y. Chen, "Wideband Spectrum Sensing for Cognitive Radio Networks: A survey," *IEEE Transactions on Wireless Communications*, vol. 20, no.2, pp 74-81, 2013. Article (CrossRef Link)

[3] W. Lu, J. Wang, "Opportunistic Spectrum Sharing Based on Full-Duplex Cooperative OFDM Relaying," *IEEE Communications Letters*, vol. 18, no. 2, pp 241-244, 2014. Article (CrossRef Link)

[4] M. Klymash, M. Jo, T. Maksymyuk, et al., "Spectral efficiency increasing of cognitive radio networks," in *Proc. of IEEE International Conference on Experience of Designing and Application of CAD Systems in Microelectronics (CADSM)*, pp 169-171, 2013. Article (CrossRef Link)

[5] E.C.Y. Peh, Y.C. Liang, Y.L. Guan, et al., "Cooperative Spectrum Sensing in Cognitive Radio Networks with Weighted Decision Fusion Scheme," *IEEE Transactions on Wireless Communications*, vol. 9, no. 12, pp 1-5, 2010. Article (CrossRef Link)

[6] E.C.Y. Peh, Y.C. Liang, Y.L. Guan, et al., "Energy-Efficient Cooperative Spectrum Sensing in Cognitive Radio Networks," in *Proc. of Global Telecommunications Conference (GLOBECOM 2011)*, pp 1-5, 2011. Article (CrossRef Link)

[7] M. Chen, L.T. Yang, T. Kwon, et al., "Itinerary Planning for Energy-Efficient Agent Communications in Wireless Sensor Networks," *IEEE Transactions on Vehicular Technology*, vol. 60, no. 7, pp 3290-3299, 2011. Article (CrossRef Link)
[8] L.N. Wang, L.I. Chao, X.W. Zhou, "Cooperative Spectrum Sensing in Cognitive Radio Networks," *Telecommunication Engineering*, vol. 62, no. 3, pp 569-580, 2008. Article (CrossRef Link)
[9] M. Haddad, Y. Hayel, O. Habachi, "Spectrum Coordination in Energy-Efficient Cognitive Radio Networks," *IEEE Transactions on Vehicular Technology*, vol. 64, no. 5, pp 2112-2122, 2015. Article (CrossRef Link)
[10] Y.C. Liang, Y. Zeng, E.C.Y. Peh, "Sensing-throughput tradeoff for cognitive radio networks," *IEEE Transactions on Wireless Communications*, vol. 7, no. 4, pp 1326-1336, 2008. Article (CrossRef Link)
[11] X. Liu, G. Bi, Y.L. Guan, et al., "Joint optimization algorithm of cooperative spectrum sensing with cooperative over-head and sub-band transmission power for wideband cognitive radio network," *Transactions on Emerging Telecommunications Technologies*, vol. 26, no. 4, pp 586-597, 2015. Article (CrossRef Link)
[12] R. Fan, H. Jiang, Q. Guo, et al., "Joint Optimal Cooperative Sensing and Resource Allocation in Multichannel Cognitive Radio Networks," *IEEE Transactions on Vehicular Technology*, vol. 60, no. 2, pp 722-729, 2011. Article (CrossRef Link)
[13] M. Jo, L. Han, D. Kim, et al., "Selfish attacks and detection in cognitive radio Ad-Hoc networks," *IEEE Network*, vol. 27, no. 3, pp 46-50, 2013. Article (CrossRef Link)
[14] G. Kramer, M. Gastpar, P. Gupta., "Cooperative Strategies and Capacity Theorems for Relay Networks," *IEEE Transactions on Information Theory*, vol. 51, no. 9, pp 3037-3063, 2005. Article (CrossRef Link)
[15] Q. Guan, F.R. Yu, S. Jiang, et al., "Capacity-Optimized Topology Control for MANETs with Cooperative Communications," *IEEE Transactions on Wireless Communications*, vol. 10, no. 7, pp 2162-2170, 2011. Article (CrossRef Link)
[16] Y. Chen, H. Huang, V.K.N. Lau, "Cooperative Spectrum Access for Cognitive Radio Network Employing Rateless Code," in *Proc. of IEEE International Conference on Communications Workshops, 2008. ICC Workshops*, pp 326-331, 2008. Article (CrossRef Link)
[17] O. Simeone, Y. Bar-Ness, U. Spagnolini, "Stable Throughput of Cognitive Radios With and Without Relaying Capability," *IEEE Transactions on Communications*, vol. 55, no. 12, pp 2351-2360, 2007. Article (CrossRef Link)
[18] R. Xie, F.R. Yu, H. Ji, "Outage capacity optimisation for cognitive radio networks with cooperative communications," *IET Communications*, vol. 6, no. 11, pp 1519-1528, 2012. Article (CrossRef Link)
[19] W. Su, J.D. Matyjas, S. Batalama, "Active Cooperation between Primary Users and Cognitive Radio Users in Heterogeneous Ad-Hoc Networks," *IEEE Transactions on Signal Processing*, vol. 60, no. 4, pp 1796-1805, 2012. Article (CrossRef Link)
[20] T. Cui, F. Gao, A. Nallanathan, "Optimization of Cooperative Spectrum Sensing in Cognitive Radio," *IEEE Transactions on Vehicular Technology*, vol. 60, no. 4, pp 1578-1589, 2011. Article (CrossRef Link)
[21] X. Liu, "A new sensing-throughput tradeoff scheme in cooperative multiband cognitive radio network," *International Journal of Network Management*, vol. 24, no. 3, pp 200-217, 2014. Article (CrossRef Link)
[22] N.C. Beaulieu, J. Hu, "A closed-form expression for the outage probability of decode-and-forward relaying in dissimilar Rayleigh fading channels," *IEEE Communications Letters*, vol. 10, no. 12, pp 813-815, 2007. Article (CrossRef Link)
[23] S. Boyd, L. Vandenberghe, "Convex Optimization," *Cambridge University Press*, 2004. Article (CrossRef Link)
[24] C. Floudas, P. M. Pardalos, "Encyclopedia of Optimization," *Springer-Verlag GmbH*, 2008. Article (CrossRef Link)

Weizhi Zhong received her M.Sc degree in communication engineering from Jilin University in 2006 and Ph.D. degree in communication engineering from Harbin Institute of Technology in 2010, respectively. She is currently a lecturer in College of Astronautics, Nanjing University of Aeronautics and Astronautics, China. Her research interests focus on broadband communications, MIMO technology and satellite communications.

Kunqi Chen received his B.E. degree in communication engineering from Nanjing University of Aeronautics and Astronautics in 2014. He is currently a graduate student in College of Astronautics, Nanjing University of Aeronautics and Astronautics, China. His research interests focus on cognitive radio, cooperative communication, spectrum resource allocation and advanced mobile communication technology for 3G and LTE.

Xin Liu received his M.Sc degree and Ph.D. degree in communication engineering from Harbin Institute of Technology in 2008 and 2012, respectively. He is currently an associate professor in the School of Information and Communication Engineering, Dalian University of Technology, China. From 2013 to 2016, he was a lecturer in the college of Astronautics, Nanjing University of Aeronautics and Astronautics, China. His research interests focus on communication signal processing, cognitive radio, spectrum resource allocation and broadband satellite communication.

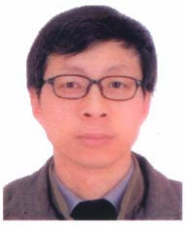

Jianjiang Zhou received his M.Sc degree and Ph.D. degree in communication engineering from Nanjing University of Aeronautics and Astronautics in 1988 and 2001, respectively. He is currently a professor in College of Electronic and Information Engineering, Nanjing University of Aeronautics and Astronautics, China. His research interests focus on radar target recognition, RF stealth and array signal processing.